ACS OMEGA

Article

Cite This: ACS Omega 2019, 4, 16171−16180

http://pubs.acs.org/journal/acsodf

Importance of the Nanofluid Preparation for Ultra-Low Interfacial Tension in Enhanced Oil Recovery Based on Surfactant−Nanoparticle−Brine System Interaction

Stefania Betancur,*[,†,‡] Lady J. Giraldo,[†] Francisco Carrasco-Marín,[‡] Masoud Riazi,[§] Eduardo J. Manrique,[∥] Henderson Quintero,[∥] Hugo A. García,[∥] Camilo A. Franco-Ariza,[†] and Farid B. Cortés[†]

[†]Grupo de Investigación en Fenómenos de Superficie—Michael Polanyi, Facultad de Minas, Universidad Nacional de Colombia Sede Medellín, Kra 80 No. 65-223, 050034 Medellín, Colombia

[‡]Grupo de Investigación en Materiales de Carbón, Departamento de Química Inorgánica, Facultad de Ciencias, Universidad de Granada, 18071 Granada, España

[§]Department of Petroleum Engineering, School of Chemical and Petroleum Eng, Shiraz University, 7134814666 Shiraz, Iran

[∥]Instituto Colombiano del Petróleo (ICP), Ecopetrol S.A., Km 7 Autopista Piedecuesta, 681011 Santander, Colombia

ABSTRACT: The main objective of this study is to evaluate the effect of the preparation of the nanofluids based on the interactions between the surfactants, nanoparticles, and brine for being applied in ultra-low interfacial tension (IFT) for an enhanced oil recovery process. Three methodologies for the addition of the salt−surfactant−nanoparticle components for the formulation of an efficient injection fluid were evaluated: order of addition (i) salts, nanoparticles, and surfactants, (ii) salts, surfactants, and then nanoparticles, (iii) surfactants, nanoparticles, and then salts. Also, the effects of the total dissolved solids and the surfactant concentration were evaluated in the interfacial tension for selecting the better formulation of the surfactant solution. Three nanoparticles of different chemical natures were studied: silica gel (SiO_2), alumina (γ-Al_2O_3), and magnetic iron core−carbon shell nanoparticles. The nanoparticles were characterized using dynamic light scattering, zeta-potential, N_2 physisorption at −196 °C, and Fourier transform infrared spectroscopy. In addition, the interactions between the surfactant, different types of nanoparticles, and brine were investigated through adsorption isotherms for the three methodologies. The nanofluids based on the different nanoparticles were evaluated through IFT measurements using the spinning drop method. The adsorbed amount of surfactant mixture on nanoparticles decreased in the order of alumina > silica gel > magnetic iron core−carbon shell nanoparticles. The minimum IFT achieved was 1×10^{-4} mN m^{-1} following the methodology II at a core−shell nanoparticle dosage of 100 mg L^{-1}.

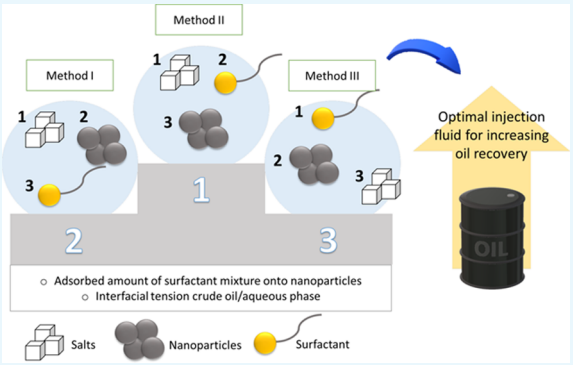

1. INTRODUCTION

The current decline in oil reserves and high energy demand worldwide leads to the continuous improvement of conventional extraction methods.[1,2] Depending on the fluids and petrophysical properties of the rock and reservoir conditions, several enhanced oil recovery (EOR) methods are used to recover as much oil as possible.[3,4] The chemical enhanced oil recovery (CEOR) methods have gained great importance and attention as their field application has increased due to the high impact on the recovery factor.[4,5] The surfactant flooding is one of the CEOR processes, which has been applied in reservoirs after applying some oil recovery methods such as waterflooding and polymer flooding.[6] The surfactant contributes to reducing the interfacial tension (IFT) between water and crude oil up to ultra-low ranges (from 10^{-3} up to 10^{-6} mN m^{-1}), alters the porous medium wettability, and consequently releases the trapped oil by capillary and interfacial forces in the porous medium.[7] However, the adsorption of the surfactant solution,[1] significantly decreases the efficiency of surfactant flooding and increases the cost of the process. This situation implies to reduce the cost/benefit ratio with the improvement of conventional EOR techniques.[8,9] Sulfonates and sulfonate/alcohol mixtures are frequently used as surfactant solutions with electrolytes to achieve interfacial tension values in the ultra-low range to significantly decrease the saturation of residual oil (<0.05).[1,3,9] However, there are different critical factors that significantly affect the process behavior such as chemical nature, surfactant concentration, salinity, temperature, and adsorption onto the porous medium.[7,10,11] Many studies have reported the use of binary and ternary surfactant

Received: July 28, 2019
Accepted: September 4, 2019
Published: September 17, 2019

DOI: 10.1021/acsomega.9b02372
ACS Omega 2019, 4, 16171−16180

mixtures in optimal formulations to promote synergistic effects for the reduction of the interfacial tension to ultra-low ranges.[7,12−15]

Recently, several authors have reported the use of nanotechnology in synergy with different conventional EOR techniques such as polymer flooding,[16−18] surfactant flooding,[15,19−21] and alkali−surfactant−polymer flooding[22,23] to increase its performance regarding areal sweep efficiency, wettability alteration, and interfacial tension for improving oil recovery. In this sense, Xu et al.[24] focused their work on the formulation of a nanofluid based on an anionic surfactant and commercial silica gel nanoparticles for obtaining ultra-low interfacial tension. All solutions were prepared with simulated formation water. The interfacial tension was reduced to values of 1×10^{-3} mN m^{-1} with a concentration of the anionic surfactant of 0.05 wt % and slightly decreased with a nanoparticle concentration of 0.01 wt % at a temperature of 90 °C. Suleimanov et al.[25] evaluated the synergistic effect of an anionic surfactant and nonferrous metal nanoparticles on the IFT reduction for enhanced oil recovery. The authors, however, did not report the use of brine in their study. The nanofluid reduced the IFT up to 10.9×10^{-3} N m^{-1} at a nanoparticle concentration of 0.001 wt % and at room temperature. Shahzad et al.[26] performed a review that discussed the use of nanoparticles in enhanced oil recovery methods. The nanofluids were prepared with nanoparticles of silica, alumina, and zirconium oxide and different types of surfactants. No ultra-low interfacial tension values were reported among the systems. The lowest interfacial tension obtained was 1.45 mN m^{-1} at a concentration of nanoparticles of 0.01 wt %. Also, Betancur et al.[27] evaluated the interactions between silica gel nanoparticles and surfactants of different chemical natures for the development of a nanofluid as an alternative CEOR method, ignoring the interactions with the brine. The nanofluid obtained based on the cationic surfactant achieved an IFT up to 5 mN m^{-1}, which is above the range of ultra-low IFT. Subsequently, Betancur et al.[28] formulated a nanofluid based on magnetic iron core−carbon shell nanoparticles and a surfactant mixture for obtaining ultra-low interfacial tension. The minimum IFT was 1×10^{-4} mN m^{-1} at a nanoparticle concentration of 100 mg L^{-1}. This behavior was related to the synergy between the free surfactant in the bulk phase and the nanoparticles with the adsorbed surfactant. It is worth mentioning that these studies did not present a defined methodology for the preparation of the nanofluid and did not consider the importance of the interactions between surfactant, nanoparticles, and brine for obtaining ultra-low interfacial tension.

There is not enough information about an efficient methodology for the preparation of a nanofluid based on the interaction between brine, surfactant, and nanoparticles for being applied in the CEOR process under conditions of ultra-low IFT. Therefore, this study examined three methodologies for the preparation of the nanofluids composed of three components (brine, surfactant, and mixture-nanoparticles) based on the order of addition to the deionized water: (I) salts, nanoparticles, and then the surfactant mixture, (II) salts, the surfactant mixture, and then nanoparticles, and (III) the surfactant mixture, nanoparticles, and salts. Adsorption isotherms were constructed to investigate the surfactant−nanoparticle interactions in the presence of brine. The experimental data of adsorption isotherms were fitted to the solid−liquid equilibrium (SLE) model. The effect of the nanofluids prepared based on the methodologies described above on the interfacial tension between crude oil and chemicals (i.e., the surfactant solution with and without nanoparticles) was investigated.

2. EXPERIMENTAL SECTION

2.1. Materials. Two commercial surfactants were employed for all experiments: an alkyl propoxy sulfate (surfactant 1 or S1) and an internal olefin sulfonate (surfactant 2 or S2) purchased from Ecopetrol S.A. using a suggested ratio (S1:S2) of 80:20. Sodium chloride (NaCl 99%, PubChem, United States), potassium chloride (KCl ≥ 99%, PubChem, United States), calcium chloride dihydrate ($CaCl_2 \cdot 2H_2O$ ≥ 99%, Sigma-Aldrich, United States), and magnesium chloride hexahydrate ($MgCl_2 \cdot 6H_2O$ ≥ 99%, Sigma-Aldrich, United States) were used for the preparation of synthetic brine solution. This brine was formulated according to the conditions of the injection water of a Colombian field. Fumed silica gel and alumina nanoparticles were purchased from Sigma-Aldrich (MO, United States) and Petroraza S.A.S (Colombia), respectively. Magnetic iron core−carbon shell nanoparticles were synthesized based on previous works.[28,29] An intermediate Colombian crude oil of 33° API was employed for the interfacial tension measurements. Crude oil had a dynamic viscosity of 117.6 cP at 25 °C, a surface tension of 32.4 mN m^{-1}, and basic sediment and water content of 0.5 wt %. The total acid number of the crude oil was 0.2 mg of KOH per gram of crude oil. The average content of saturated, aromatics, resins, and asphaltenes (SARA) fraction was determined through an Iatroscan MK-6 thin layer chromatograph following the IP 469 method.[30] The average content of SARA fractions were 53.9, 26.2, 12.2, and 7.7% for saturated, aromatics, resins, and asphaltenes, respectively.

2.2. Methods. *2.2.1. Nanoparticle Characterization.* The nanoparticles were characterized using Fourier transform infrared spectroscopy (FTIR) with an infrared spectrometer IRAffinity—1S (Shimadzu Corporation, Japan) for chemical composition identification, dynamic light scattering (DLS), and zeta-potential using a nanoplus-3 (Micromeritics, United States) for particle size and pH of the isoelectric point determination, respectively. N_2 adsorption isotherms were obtained at −196 °C with a Gemini VII 2390 specific surface analyzer (Micromeritics, United States) for surface area (S_{BET}) determination. For FTIR tests, KBr solution was used with a KBr/nanoparticle ratio of 30:1 % w/w. For measurements, 15 sweeps per minute were taken for each sample in the range of 600−4000 cm^{-1} at a resolution of 2 cm^{-1}. For the DLS measurements, the nanoparticles were previously dispersed in deionized water at a concentration below 50 mg L^{-1} and then were subjected to ultrasound at room temperature for 4 h. The mean particle size was estimated from the Stokes−Einstein equation.[31,32] For physisorption of N_2, the nanoparticles were degassed for 12 h under vacuum conditions (6^{-10} mbar). Surface area values (S_{BET}) were calculated by the Brunauer−Emmett−Teller (BET) method.[33] For determining the pH of the isoelectric point, a specific dry mass of each nanoparticle type was added to different samples of deionized water with varying solution pH from 2 to 12. The solutions were stirred at 600 rpm for 24 h.[34] Then, the zeta-potential of each sample was measured using a nanoplus-3 (Micromeritics, United States). The measured zeta potential was plotted against the pH. The intersection point of the obtained curve with the abscissa axis is the pH of the isoelectric point.

DOI: 10.1021/acsomega.9b02372
ACS Omega 2019, 4, 16171−16180

2.2.2. Preparation and Characterization of the Surfactant Mixture. Interfacial tension measurements were performed to select the total dissolved solid (TDS %) percentage for the preparation of the synthetic brine, which was used in all experiments. The synthetic brine solutions were prepared at TDS percentages between 0.1 and 2.5%. The brine employed was selected based on a characteristic injection brine of a Colombian field. S1 and S2 surfactants were used for the preparation of the surfactant mixture. Similarly, the surfactant concentration was selected based on the interfacial tension behavior between the crude oil and the surfactant at different concentrations. For the preparation of the surfactant mixture, S1 was first added to the brine (previously prepared) followed by S2. The surfactant formulation was characterized using FTIR, critical micelle concentration (CMC), and hydrophilic−lipophilic balance (HLB) determination. The CMC of the surfactant mixture was approximately 1800 mg L^{-1} according to a previous study.[28] The analysis of FTIR for a liquid surfactant sample[35] was performed using the 2-propanol standard with an infrared spectrometer IRAffinity 1-S (Shimadzu Corporation, Japan) at atmospheric conditions. Ten sweeps per minute were taken for each sample in the range of 600−4000 cm^{-1} at a resolution of 1 cm^{-1}. The measurement of HLB of the surfactant mixture was performed following the method proposed by Chun et al.[36] based on interfacial tension measurements. Interfacial tension experiments were performed between the aqueous solution with the surfactant mixture and crude oil at 25 °C. Each measurement was made in triplicate to ensure the reproducibility of the measurements. For the interfacial tension measurements, a Du Noüy tensiometer (Krüss, Germany)[37] provided with a platinum−iridium ring was used. The HLB value was calculated based on eq 1[36]

$$\mathrm{HLB} = \frac{-(\gamma - 45.7)}{2.36} \tag{1}$$

where γ is the interfacial tension measurement between the aqueous solution with the surfactant mixture and toluene.

2.2.3. Interaction Methodologies: Order of Addition. For the preparation of nanofluids, it is very important to understand the brine−surfactant−nanoparticle interactions. Thus, three different methodologies were employed for the preparation of nanofluids to determine an optimal procedure to prepare the nanofluid. The following procedures were evaluated: (I) the addition of the salts to the deionized water, followed by the addition of the dry powder nanoparticles, and then the surfactant mixture (surfactant S1 was first added to the water and then surfactant S2 was added), (II) the salts are dissolved in the deionized water followed by the surfactant mixture, and finally the dry powder nanoparticles are added, and (III) first, the surfactant mixture (surfactant S1 was first added to the water and then surfactant S2 was added) is added to the deionized water followed by the dry powder nanoparticles, and then the salts were added. Each prepared solution was magnetically stirred for 2 h and left to stand for 24 h before the tests to allow the interactions between brine, nanoparticles, and the surfactant mixture. These procedures will allow producing a nanofluid with better properties for being used in the CEOR process.

2.2.4. Adsorption Isotherms. The adsorption tests of surfactant formulation onto different nanoparticle types were performed based on previous works.[27] These materials have not been applied in CEOR processes at ultra-low IFT. The experiments were conducted at atmospheric pressure by fixing the concentration of the surfactant mixture and varying the dosage of the nanoparticles between 100 and 1000 mg L^{-1}. The surfactant concentration was selected with the lowest value of IFT at the different concentrations evaluated. For the experiments, nanoparticles of different chemical natures were used: silica gel, alumina, and magnetic iron core−carbon shell nanoparticles. The preparation of each solution was performed based on the three preparation methodologies previously described. The adsorption experiments were performed through thermogravimetric analyses with a TGA analyzer (Q50, TA Instruments Inc., New Castle, DE). The nanoparticles with the adsorbed surfactant onto their surface were heated in air from 30 to 800 °C at 20 °C min^{-1} and a constant airflow rate of 100 mL min^{-1}. Also, the experimental data were fitted by the solid−liquid equilibrium (SLE) model, which is based on the adsorption theory of self-associative molecules over a solid surface. The SLE model is described as follows

$$C_E = \frac{\psi H}{1 + K\psi} \exp\left(\frac{\psi}{q_m}\right) \tag{2}$$

$$\psi = \frac{-1 + \sqrt{1 + 4K\xi}}{2K} \tag{3}$$

$$\xi = \left(\frac{q_m \cdot q}{q_m - q}\right) \tag{4}$$

where q (mg g^{-1}) is the amount of the surfactant adsorbed onto nanoparticles, q_m (mg g^{-1}) is the maximum adsorption capacity, C_E (mg g^{-1}) is the equilibrium concentration of the surfactant in the solution, K (g g^{-1}) is an indicator of the association of surfactant molecules, and H is the measured Henry's law constant and is an indicator of affinity between the adsorbate and the adsorbent. Additional details about the SLE model can be found in previous works.[27,38] All measurements were performed in triplicate to ensure reproducibility. The uncertainties were shown as error bars in adsorption isotherms. The errors were calculated through the root-mean-square error (RMS %)[27] as follows

$$RMS\% = \sqrt{\frac{\sum_{i=1}^{m} (C_{experimental,i} - C_{model,i})^2}{m}} \times 100 \tag{5}$$

2.2.5. Interfacial Tension Measurements. The IFT measurements were performed for nanoparticles of different chemical natures at 52 °C and atmospheric pressure. For the experiments, a spinning drop tensiometer (Grace Instrument, United States) was used by adding a drop of crude oil to the aqueous phase with the surfactant mixture and the different types of nanoparticles at concentrations between 10 and 1000 mg L^{-1}.[39,40] The interfacial tension value is determined when the system is in equilibrium by the Vonnegut equation[41] as follows

$$\gamma = 1.44e - 7 \cdot \Delta\rho \cdot D^3 \cdot \theta^2 \tag{6}$$

where $\Delta\rho$ (g mL^{-1}) is the density difference of the fluids, θ (rpm) is the angular velocity, D (mm) is the diameter of the oil phase drop and γ (mN m^{-1}) is the interfacial tension between the fluid with nanoparticles and crude oil. All of the measurements were performed by triplicate.

DOI: 10.1021/acsomega.9b02372
ACS Omega 2019, 4, 16171−16180

3. RESULTS AND DISCUSSION

3.1. Characterization of the Nanoparticles and Surfactant Mixture.

Table 1 shows the mean particle size of nanoparticles, determined through DLS measurements and estimated the BET surface area using physisorption of N_2 at −196 °C. As expected, the smaller the mean particle size of nanoparticles, the larger the surface area. This behavior occurs mainly for nonporous materials, as the carbon shell of the nanoparticles.[42] Indeed, silica gel nanoparticles present the smallest size (7 nm) and the largest surface area among the nanoparticles (389 $m^2\ g^{-1}$).

Table 1. Estimated BET Surface Area and Mean Particle Size of Nanoparticles

material	mean particle size (nm)	BET surface area ($m^2\ g^{-1}$)
silica gel	7	389
alumina	35	223
core−shell	60	123

The functional groups present in silica gel, alumina, and magnetic iron core−carbon shell nanoparticles were verified using FTIR, which is shown in Figure 1. The FTIR spectra of

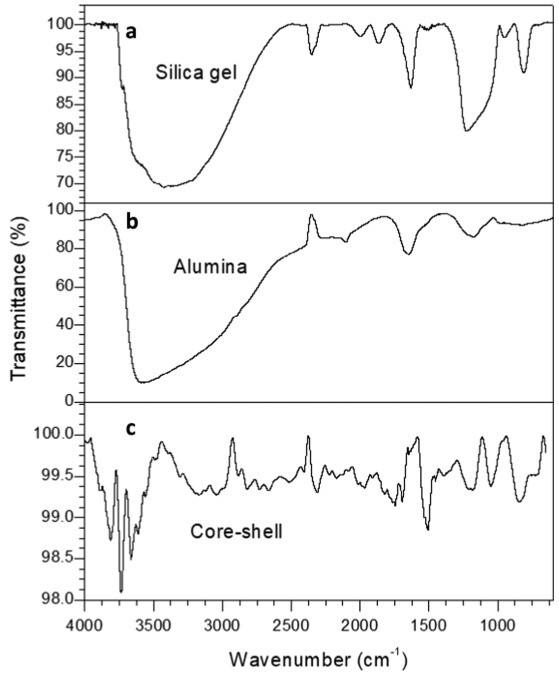

Figure 1. FTIR spectra of (a) silica gel, (b) alumina, and (c) magnetic iron−carbon shell nanoparticles.

silica gel nanoparticles (Figure 1a) present characteristic bands at the 3200−3700 cm^{-1} range corresponding to Si−OH. Si−H vibration produces a band at the 2250 cm^{-1} region and strong vibrations of the Si−O−Si siloxane structure show characteristic infrared bands at 1570 cm^{-1}. Vibrations of $Si(CH_3)$ appear in the region near 1250 cm^{-1} and Si−H produces a band in the 800−985 cm^{-1} range.[43] Similarly, the FTIR spectra of alumina nanoparticles were obtained (Figure 1b). The band near 3600 cm^{-1} is associated with the stretching vibration of hydroxyl groups (O−H), which can be due to the presence of water in the sample.[34,44] Another characteristic infrared band appears near 1600 cm^{-1}, corresponding to the vibration of CO_2 (impurity).[45,46] The octahedral structure Al-O_6 produced a band near 1070 cm^{-1}.[47] All of the structures showed in FTIR spectra of alumina are related to the characteristic functional groups of this material. Finally, the FTIR spectra of magnetic iron core−carbon shell nanoparticles are shown in Figure 1c. It is observed that the characteristic infrared bands in the region 3000−3600 cm^{-1} are associated with O−H and N−H vibrations.[48] The secondary amide N−H stretching could be related to the use of urea (carbamide) during nanoparticle synthesis. C−H stretching appears at the 2800−3000 cm^{-1} region, which can be associated with aromatic structures of pyrocatechol. C═O stretching produces bands at the 1650−1770 cm^{-1} region. The presence of the carbonyl group can be associated with the use of urea for synthesis or resulted from the carbonization of the polymeric network during the hydrothermal process.[49] C═C stretching appears in the 1500−1700 cm^{-1} region, which is related to aromatic structures. C−O stretching is observed in the 1200−1300 cm^{-1} and 1050−1060 cm^{-1} ranges. C−H stretching produces a band near 830 cm^{-1}, which is related to the presence of aromatic structures.[50] Additional details regarding the synthesis and characterization of magnetic iron core−carbon shell nanoparticles can be found in previous works.[28]

Figure 2 presents the infrared spectra of two surfactants selected for all experiments: an alcohol propoxy sulfate (S1)

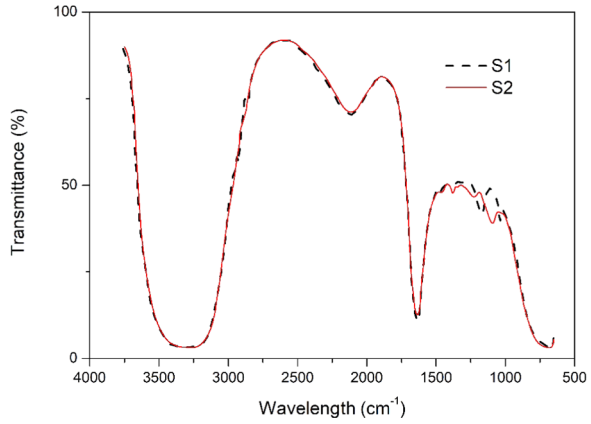

Figure 2. FTIR spectra for surfactants S1 and S2.

and an internal olefin sulfonate (S2). The surfactants S1 and S2 have hydrophilic and hydrophobic character, respectively. The continuous line corresponds to surfactant S1 and the dashed line to surfactant S2. As observed, the infrared spectra for S1 and S2 show similar characteristic bands. O−H stretching appears at 3300 cm^{-1}. Both surfactants show characteristic infrared bands of aliphatic compounds corresponding to the hydrophobic carbon chain of the surfactant molecule. C−H stretching vibrations occur near 3000−3100 cm^{-1} and produces characteristic bands at the 2200−2450 cm^{-1} region.[43] Similarly, CH_3 and CH_2 vibrations could be related to the bands at the 1400−1470 cm^{-1} range. However, the infrared spectra for S1 and S2 present some differences. The infrared spectra of the S1 surfactant present a band near 1105 cm^{-1}, which is associated with SO_4^{2-} vibration.[51] The SO_4^{2-} structure corresponds to the hydrophilic group of the S1 surfactant molecule. The infrared spectra of the S2 surfactant show characteristic bands at 1620−1680 cm^{-1} corresponding to C═C vibration. C═C vibration belongs to the frequency group of olefins (alkenes).[52] At the same time, the olefin is

DOI: 10.1021/acsomega.9b02372
ACS Omega 2019, 4, 16171−16180

associated with the hydrophobic chain of the S2 molecule. SO_3^{2-} vibration appears near 967 cm^{-1},[51] which belongs to the hydrophilic group of the S2 surfactant molecule.

3.2. Effect of the TDS and Surfactant Mixture Concentration on IFT Data. Salinity is one of the most important parameters associated with the occurrence of an ultra-low interfacial tension.[11] Interfacial tension measurements were performed between an intermediate crude oil and synthetic brine with total dissolved solids[53] (TDS %) at concentrations between 0.1 and 2.5% at 52 °C and atmospheric pressure. The temperature was selected based on previous work[28] and it is within the range of temperatures used commonly in surfactant flooding performed at the field scale.[54] The synthetic brine was prepared based on a specific Colombian formulation. These experiments were performed to choose an optimum salinity for adsorption experiments and IFT tests. As observed in Figure 3, the IFT between the crude oil and synthetic brine with 0.785% of TDS was the lowest among the evaluated concentrations. Therefore, a synthetic brine with 6.46 g L^{-1} of NaCl, 0.136 g L^{-1} of KCl, 1.05 g L^{-1} of $CaCl_2{\cdot}2H_2O$, and 0.20 g L^{-1} of $MgCl_2{\cdot}6H_2O$, for a TDS of 0.785%, was used for all experiments. On the other hand, IFT measurements were performed to select the concentration of the surfactant mixture at which the lowest interfacial tension is obtained. For IFT experiments, the 80:20 ratio between the surfactant S1 and S2 remained constant. The IFT results were 4.5×10^{-3}, 1.4×10^{-3}, and 2.2×10^{-4} mN m^{-1} for mass fractions of the surfactant mixture of 0.15, 0.18, and 0.2%, respectively. In agreement with these results, the mass fraction of 0.2% (2000 mg L^{-1}) was selected as a surfactant mixture concentration for all experiments. The interfacial tension of a system that contains a surfactant does not change significantly upon reaching its critical micelle concentration (CMC). The CMC of the surfactant mixture was approximately 1800 mg L^{-1},[28] i.e., above this concentration, an excess of micelles does not change the interfacial activity of the system. This situation corroborates the selection of 2000 mg L^{-1} as an adequate surfactant concentration.

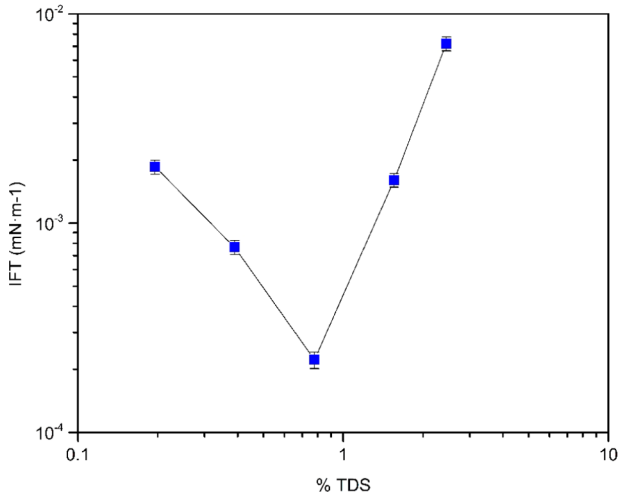

Figure 3. Interfacial tension between the crude oil and synthetic brine with different TDS percentages at a fixed temperature of 52 °C.

3.3. Adsorption Isotherms. Figure 4 shows the adsorption isotherms for the surfactant mixture of S1 and S2 onto nanoparticles of different chemical natures at 25 °C. For the adsorption experiments, different masses of nanoparticles were added to the brine with a fixed concentration of the surfactant mixture of 2000 mg L^{-1}. This surfactant concentration is above the critical micelle concentration (CMC), which was approximately 1800 mg L^{-1}.[28] The adsorption isotherms were constructed based on the preparation methods I, II, and III. As observed in Figure 4, the adsorbed amount of surfactant decreased in the following order: method II > method I > method III. In method II, the surfactant mixture is added to the brine solution before the nanoparticles. The presence of electrolytes generates a higher concentration around the surfactant molecules, which promote the reduction of electrostatic forces between the charged hydrophilic components of surfactants, favoring the formation of micelles.[55] Thus, the surfactant is probably adsorbed onto nanoparticles as micelles.[27] This situation is evidenced in the adsorbed amount of the surfactant onto nanoparticles, which is the highest among the evaluated methods. For method I, the nanoparticles are added to the brine solution before the surfactant mixture. This behavior suggests that electrolytes could be interacting with the charged surface of the nanoparticles.[56] Then, when the surfactant mixture is added

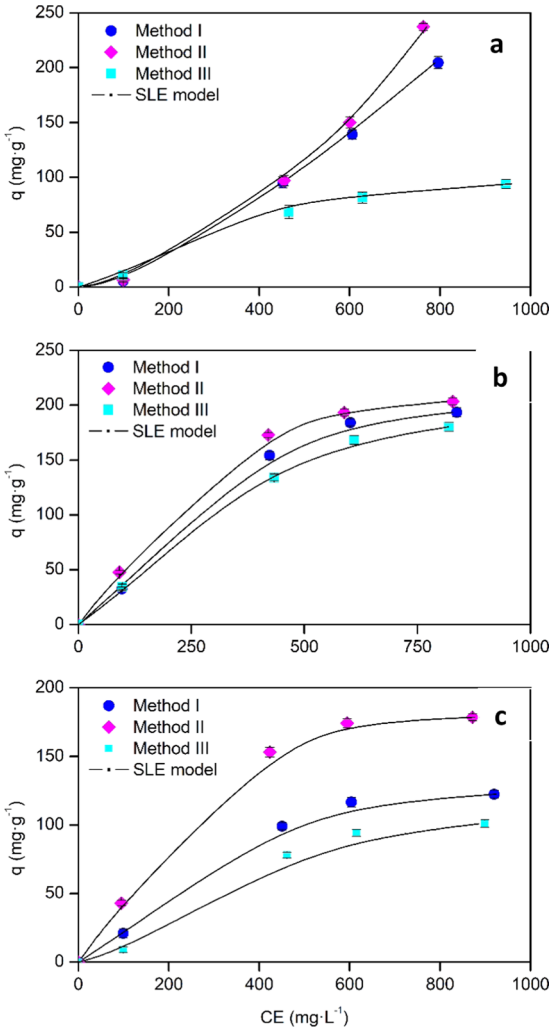

Figure 4. Adsorption isotherms for the surfactant mixture of S1 and S2 at a fixed concentration of 2000 mg L^{-1} onto (a) magnetic iron core−carbon shell, (b) alumina, and (c) silica gel nanoparticles at 25 °C using Methods I, II, and III. The symbols are from the experimental data, and the continuous lines are from the SLE model.

DOI: 10.1021/acsomega.9b02372
ACS Omega 2019, 4, 16171−16180

to the aqueous phase, there are less free electrolytes that favor the formation of surfactant micelles. Therefore, the adsorbed amount of surfactant onto nanoparticles is lower for method I than method II. For method III, the salts were added after the addition of the surfactant mixture and the nanoparticles. In this case, the salts did not have the same effect on the formation of surfactant micelles as in the case of method I or II. This behavior suggests that the surfactant can be adsorbed on the surface of the nanoparticles as molecules. Therefore, method III shows the lowest adsorbed amount of surfactant onto nanoparticles.

On the other hand, as observed in Figure 4, the amount of adsorbed surfactant decreased in the following order: alumina > silica gel > magnetic iron core−carbon shell nanoparticles. All solutions for adsorption isotherm construction presented a pH of approximately 7. For pure silica gel and alumina nanoparticles, the pH of the isoelectric point was close to 2 and 9.9, respectively.[34] For magnetic iron core−carbon shell nanoparticles, the measured pH of the isoelectric point was 2.4. This behavior suggests that silica gel and magnetic iron core−carbon shell nanoparticles in a solution with a pH of 7 present a negatively charged surface. In contrast, alumina nanoparticles in a solution of a pH lower than the pH of the isoelectric point are positively charged. In this way, the positive charges of alumina nanoparticles and the sulfate and sulfonate anions of surfactants S1 and S2, respectively, generate electrostatic attractive interactions. These surfactant−nanoparticle interactions favor the adsorption of surfactants onto surface nanoparticles. The negative charges of silica gel and core−shell nanoparticles make it difficult for the surfactant molecules to get adsorbed onto nanoparticles, which is evidenced in the adsorbed amount obtained for each nanoparticle type.

For all cases, alumina and silica gel nanoparticles showed type I (a) adsorption isotherm behavior according to the International Union of Pure Applied Chemistry (IUPAC) scheme.[57] However, magnetic iron core−carbon shell nanoparticles showed type III isotherm behavior using Methods I and II but presented a type I (a) isotherm behavior when the nanofluid was prepared through method III. Type I (a) isotherm indicates that the adsorbate is adsorbing onto the adsorbent surface in a monolayer. Type III isotherm behavior is characterized by low adsorbate−adsorbent affinities.[57] The hydrophilic−lipophilic balance (HLB) of the surfactant mixture of S1 and S2 was 18. This value indicates that the surfactant mixture presents high solubility in water;[58] i.e., the surfactant mixture has a polar character. Likewise, it is known that carbon also has a hydrophilic/hydrophobic character.[59] Therefore, type III adsorption behavior for magnetic iron core−carbon shell nanoparticles can be related to the interactions between the hydrophobic groups of the nanoparticle surface and the polar character of the surfactant mixture. This situation is in agreement with the low adsorbate−adsorbent affinities that characterize the type III adsorption isotherm. For Methods I and II, the salts favor the hydrophobic interactions among the lipophilic groups of the surfactant molecules; i.e., the presence of salts favors the surfactant−surfactant interactions. The hydrophobic groups of the surface of nanoparticles and the polar surfactant mixture disfavor the surfactant−nanoparticle surface interactions. In this way, the surfactant−surfactant interactions could be stronger than the surfactant−nanoparticle surface interactions. Then, the surfactants could be adsorbed on the surface of the nanoparticles as aggregates. Similarly, the presence of monovalent or divalent cations of the synthetic brine could neutralize the negative charges on the surface of the nanoparticles and then the mixture of surfactants is adsorbed on the nanoparticles. Type III adsorption behavior could also be related to the adsorption of surfactant molecules by the lipophilic group. Magnetic iron core−carbon shell nanoparticles present hydrophobic groups in the surface, which would favor the adsorption of surfactant molecules by their lipophilic group in multilayers.

For method III, the salts are added to the deionized water after the surfactant mixture and the nanoparticles. The salts do not favor the hydrophobic interactions among the lipophilic groups of the surfactant molecules. This situation could hinder the surfactant−surfactant interactions and favor the surfactant−nanoparticle surface interactions. If the surfactant−nanoparticle surface interactions are stronger than the surfactant−surfactant interactions, the surfactant mixture could be adsorbed as molecules. Then, type I (a) adsorption behavior is obtained.

Type I (a) adsorption isotherms of the surfactant mixture onto alumina and silica gel nanoparticles following Methods I, II, and III were obtained. Both types of nanoparticles are polar as the surfactant mixture. In this case, the surfactant−surfactant interactions could be weaker than the surfactant−nanoparticle surface interactions. As surfactant−nanoparticle interactions could be stronger, the surfactants are adsorbed on the nanoparticles as molecules. Therefore, type I (a) isotherm behavior was obtained for alumina and silica gel nanoparticles.

Table 2 summarizes the estimated parameters of SLE model for the surfactant mixture of S1 and S2 at a fixed concentration of 2000 mg L^{-1} onto the magnetic iron core−carbon shell, alumina, and silica gel nanoparticles at 25 °C following Methods I, II, and III for the preparation of the nanofluid. As observed, the H parameter, which is an indicator of adsorption affinity of the surfactant onto nanoparticles[60] increases (i.e., adsorption affinity decreases) in the order: method II < method I < method III. The nanofluids prepared through method II present the highest adsorption affinity of adsorbate−adsorbent among the evaluated methods. The maximum adsorption capacity parameter q_{max} decreased in the order: method II > method I > method III. These results are in agreement with the adsorbed amount of surfactant onto the surface of nanoparticles observed in the adsorption isotherms of Figure 4. Similarly, the trend of the K parameter, related to

Table 2. Parameters Estimated from the SLE Model for the Surfactant Mixture of S1 and S2 onto the Magnetic Iron Core−Carbon Shell, Alumina, and Silica Gel Nanoparticles at 25 °C Using Preparation Methods I, II, and III

		parameter			
nanoparticle type	method	H (mg g^{-1})	K (g g^{-1})	q_{max} (mg g^{-1})	R^2
core−shell	I	0.021	0.049	251	0.995
	II	0.017	0.033	295	0.999
	III	0.028	0.034	107	0.993
alumina	I	0.004	0.016	218	0.996
	II	0.002	0.009	240	0.998
	III	0.005	0.015	211	0.997
silica gel	I	0.008	0.034	132	0.988
	II	0.004	0.015	205	0.982
	III	0.011	0.042	118	0.994

DOI: 10.1021/acsomega.9b02372
ACS Omega 2019, 4, 16171−16180

the self-association of the molecules of the surfactant, is in agreement with the adsorbed amount of surfactant onto nanoparticles. The adsorption experiments suggest that a formulation of nanofluid must be performed following method II. These results are in agreement with the results reported by Betancur et al.,[27] who studied the adsorption of different types of surfactants onto silica gel nanoparticles.

3.4. Interfacial Tension Experiments. Surfactant flooding is a chemical enhanced oil recovery method to reduce the interfacial tension (IFT) between the crude oil and water and/or alter the wettability of porous medium and thereby increase the oil recovery.[9] For this reason, the interfacial tension is one of the most important parameters to evaluate the performance of a new fluid used in the surfactant-based EOR process. For a successful surfactant flooding, the oil and gas industry considers that the IFT must be less than 1×10^{-2} mN m^{-1}.[7,61] The aqueous phase was prepared with the synthetic brine used for all of the experiments (TDS % of 0.785) and the surfactant mixture at a concentration of 2000 mg L^{-1}. In addition, each type of nanoparticle mentioned above was added to the solutions at dosages between 100 and 1000 mg L^{-1}. The IFT measurements were performed at a reservoir temperature of 52 °C and atmospheric pressure. The temperature is within the range of temperatures used in the Colombian field of study.[54] As observed in Figure 5, the IFT between the crude oil and the aqueous phase with a surfactant mixture of S1 and S2 (dashed line) was 2.2×10^{-4} mN m^{-1}. It is observed that the IFT values decreased in the order: method III > method I > method II for all of the nanoparticles evaluated. For methods I and II with all nanoparticle types

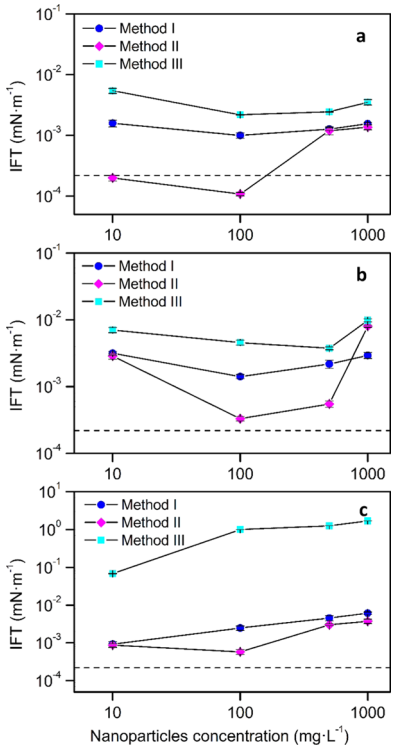

Figure 5. Interfacial tension between crude oil/synthetic brine with the surfactant mixture of S1 and S2 at 2000 mg L^{-1} (dashed line) in the absence and presence of (a) the magnetic iron core−carbon shell, (b) alumina, and (c) silica gel nanoparticles at dosages between 10 and 1000 mg L^{-1} and at a fixed temperature of 52 °C.

achieved IFT values below 1×10^{-2} mN m^{-1} within the range of nanoparticle concentrations evaluated. When the nanofluid was prepared based on method I, the nanoparticles were added to the aqueous phase after the addition of the salts but before the addition of the surfactant mixture. Then, the electrolytes interact with the charges of the nanoparticle surface and there are less available electrolytes that can favor the formation of micelles of the surfactant and facilitate the displacement of the surfactant to the interface crude oil/aqueous phase. Therefore, the IFT value is higher than that obtained with the surfactant mixture (S1 and S2) only.

For method II, the salts are added to the aqueous phase before the addition in the order of the surfactant mixture and nanoparticles. The salts favor the formation of surfactant micelles, which are adsorbed onto the surface of the nanoparticles. In this case, IFT values below the base system (surfactant mixture of S1 and S2) were obtained only for the magnetic iron core−carbon shell nanoparticles at a nanoparticle concentration ≤ 100 mg L^{-1} (Figure 5a). The reduction of IFT can be due to the synergy between the free surfactant in the bulk phase and the nanoparticles with the adsorbed surfactant onto their surface.[28] At this dosage of nanoparticles, there is enough free surfactant to reduce the IFT crude oil/aqueous phase. The IFT reduction is associated with the weakening of the interaction forces of the interface molecules. These interactions can be Debye forces or Keesom forces as was described in the previous work.[28] Likewise, it is observed that at nanoparticle dosage of 10 mg L^{-1}, the IFT value was similar to that obtained with the surfactant mixture (dashed line) but did not achieve a lower value than that obtained at 100 mg L^{-1}. At a dosage of 10 mg L^{-1} of nanoparticles, most of the surfactants are free in the continuous phase. Therefore, the nanoparticles with the adsorbed surfactant do not achieve a significant effect on interfacial phenomena of the aqueous phase/crude oil system. In contrast, at nanoparticle dosages of 500 and 1000 mg L^{-1} ultra-low interfacial tension values were not achieved. At these concentrations, the nanoparticles can adsorb a higher amount of surfactant from the bulk phase and therefore the IFT cannot be significantly reduced.[62] This behavior is in agreement with the adsorbed amount of surfactant onto nanoparticles observed in adsorption isotherms (Figure 4), where the highest adsorbed amount was obtained with method II. Similarly, for the case of magnetic iron core−carbon shell nanoparticles, Table 2 shows that the H parameter, which is associated with the affinity between the adsorbate and the adsorbent, was lower for method II than those for methods I and III. This behavior indicates that the affinity between the surfactant and the nanoparticles is higher when the nanofluid was prepared following method II. Therefore, if the the surfactant−nanoparticle affinity is strong, the surfactant keeps adsorbed onto the nanoparticle surface when they come into contact with the crude oil. Then, the reduction on IFT could be related to the order of free surfactants and nanoparticles with the adsorbed surfactant at the interface, which in this case remains adsorbed when in contact with the crude oil. Additionally, for the mentioned nanoparticles, q_{max} for method II is the highest among the evaluated methods, which is in agreement with the observed behavior.

In contrast, method III presented the highest values of IFT among the evaluated systems. For method III, the salts were added to the aqueous phase after the surfactant mixture and nanoparticle addition. In this case, the absence of salts at the

DOI: 10.1021/acsomega.9b02372
ACS Omega 2019, 4, 16171−16180

time of the addition of the surfactant mixture could disfavor the formation of micelles. Then, the surfactants are adsorbed onto the nanoparticle surface as monomers resulting in fewer surfactant molecules for the micellization process. This behavior is in agreement with the type I (a) isotherm obtained through adsorption experiments. In this way, the surfactant did not achieve optimal conditions for the reduction of IFT to ultra-low values. For example, for magnetic iron core−carbon shell nanoparticles, Table 2 showed for method III, the highest H parameter among the evaluated methods. This could be attributed to the low affinity between the surfactant and the surface of the nanoparticles when the nanofluid was prepared through method III. In this case, the low affinity between the surfactant and the surface of the nanoparticles would favor the desorption of the surfactant when the treatment contacts the crude oil. In this way, the structures located at the interface could be free surfactant from the continuous phase and the surfactant that could be desorbed from the surface of nanoparticles. Therefore, there is no synergy between the free surfactant of the bulk phase and the nanoparticles with the adsorbed surfactant, and the reduction of IFT is not significant.

4. CONCLUSIONS

Three methodologies for the preparation of a nanofluid based on brine−surfactant−nanoparticles were evaluated for the reduction of IFT of a given crude oil/aqueous phase system. The adsorbed amount of surfactant mixture onto the surface of nanoparticles decreased in the following order: method II > method I > method III and also decreased in the order alumina > silica gel > magnetic iron core−carbon shell nanoparticles. Alumina and silica gel nanoparticles showed type I (a) isotherms for the three preparation methodologies, while core−shell nanoparticles presented type III adsorption behavior for methods I and II but type I (a) adsorption isotherm for method III.

The surfactant−nanoparticle−brine interactions were in agreement with the interfacial crude oil/aqueous phase behavior. When the nanofluid was prepared following method II, the lowest interfacial tension values were obtained for all types of nanoparticles. Meanwhile, method III showed the highest IFT values among the evaluated methodologies. The nanofluid prepared through method II with a nanoparticle dosage of 100 mg L^{-1} reduced the IFT to 1×10^{-4} mN m^{-1}. This behavior is related to the synergy between the free surfactant in the bulk phase and the nanoparticles with the adsorbed surfactant. Through this work, it was demonstrated that the methodology for the preparation of a nanofluid is a key factor to maintain ultra-low interfacial tension in surfactant formulation to enhance oil recovery processes. Likewise, the understanding of the interactions of nanofluid components allows designing an injection fluid with the desired properties for a specific target.

AUTHOR INFORMATION

Corresponding Author

*E-mail: sbetancurm@unal.edu.co. Phone: +57 (4) 4255137.

ORCID

Stefania Betancur: 0000-0002-9388-9843
Francisco Carrasco-Marín: 0000-0002-2516-7806
Masoud Riazi: 0000-0003-0572-1766
Camilo A. Franco-Ariza: 0000-0002-6886-8338
Farid B. Cortés: 0000-0003-1207-3859

Notes

The authors declare no competing financial interest.

ACKNOWLEDGMENTS

Stefanía Betancur wants to acknowledge the Departamento Administrativo de Ciencia, Tecnologia e Innovación de Colombia (COLCIENCIAS) for the scholarship received from call 727−2015. The authors also acknowledge Universidad Nacional de Colombia, Universidad de Granada, agreement 3010388 of 2017 with Ecopetrol S.A., agreement 064 of 2018 with COLCIENCIAS and Agencia Nacional de Hidrocarburos (ANH), Spanish Ministry of Science, Innovation and Universities, FEDER, contract number RTI2018-099224-B-I00 and Junta de Andalucía ref RNM-172 for the support provided.

REFERENCES

(1) Thomas, S. Enhanced oil recovery-an overview. *Oil Gas Sci. Technol.* **2008**, *63*, 9−19.

(2) Al-Mjeni, R. A.-M.; Arora, S.; Cherukupalli, P. K.; Wunnik, J. N. M. V.; Edwards, J.; Felber, B. J.; Gurpinar, O.; Hirasaki, G. J.; Miller, C. A.; Jackson, C.; Kristensen, M. R.; Lim, F.; Ramamoorthy, R. Has the time come for EOR? *Oilfield Rev.* **2010**, *22*, 16−35.

(3) Sharma, T.; Iglauer, S.; Sangwai, J. S. Silica nanofluids in an oilfield polymer polyacrylamide: interfacial properties, wettability alteration, and applications for chemical enhanced oil recovery. *Ind. Eng. Chem. Res.* **2016**, *55*, 12387−12397.

(4) Manrique, E. J.; Thomas, C. P.; Ravikiran, R.; Izadi Kamouei, M.; Lantz, M.; Romero, J. L.; Alvarado, V. In *EOR: Current Status and Opportunities*, SPE Improved Oil Recovery Symp., 18th; Society of Petroleum Engineers, 2010.

(5) Sharma, T.; Sangwai, J. S. Silica nanofluids in polyacrylamide with and without surfactant: Viscosity, surface tension, and interfacial tension with liquid paraffin. *J. Pet. Sci. Eng.* **2017**, *152*, 575−585.

(6) Green, D. W.; Willhite, G. P. *Enhanced oil recovery. Henry L. Doherty Memorial Fund of AIME*; Society of Petroleum Engineers Richardson: TX, 1998; Vol. *6*.

(7) Rosen, M. J.; Wang, H.; Shen, P.; Zhu, Y. Ultralow interfacial tension for enhanced oil recovery at very low surfactant concentrations. *Langmuir* **2005**, *21*, 3749−3756.

(8) Kumar, N.; Mandal, A. Surfactant Stabilized Oil-in-Water Nanoemulsion: Stability, Interfacial Tension, and Rheology Study for Enhanced Oil Recovery Application. *Energy Fuels* **2018**, *32*, 6452−6466.

(9) Hirasaki, G.; Miller, C. A.; Puerto, M. Recent advances in surfactant EOR. *Soc. Pet. Eng. J.* **2011**, *16*, 889−907.

(10) Negin, C.; Ali, S.; Xie, Q. Most common surfactants employed in chemical enhanced oil recovery. *Petroleum* **2017**, *3*, 197−211.

(11) Fuseni, A.; Han, M.; Al-Mobith, A. *Phase Behavior and Interfacial Tension Properties of an Amphoteric Surfactant for EOR Application*, SPE Saudi Arabia Section Technical Symposium and Exhibition; Society of Petroleum Engineers, 2013.

(12) El-Batanoney, M.; Abdel-Moghny, T.; Ramzi, M. The effect of mixed surfactants on enhancing oil recovery. *J. Surfactants Deterg.* **1999**, *2*, 201−205.

(13) Comelles, F.; Sánchez-Leal, J.; Gonzalez, J. Influence of ionic surfactants on the formation of liquid crystals in oleic acid/glycol/water systems. *J. Surfactants Deterg.* **2007**, *10*, 137−144.

(14) Salager, J. L.; Forgiarini, A. M.; Bullón, J. How to attain ultralow interfacial tension and three-phase behavior with surfactant formulation for enhanced oil recovery: a review. Part 1. Optimum formulation for simple surfactant−oil−water ternary systems. *J. Surfactants Deterg.* **2013**, *16*, 449−472.

(15) Salager, J. L.; Forgiarini, A. M.; Márquez, L.; Manchego, L.; Bullón, J. How to attain an ultralow interfacial tension and a three-phase behavior with a surfactant formulation for enhanced oil recovery: a review. Part 2. Performance improvement trends from

DOI: 10.1021/acsomega.9b02372
ACS Omega 2019, 4, 16171−16180

Winsor's premise to currently proposed inter-and intra-molecular mixtures. *J. Surfactants Deterg.* **2013**, *16*, 631−663.
(16) Giraldo, L. J.; Giraldo, M. A.; Llanos, S.; Maya, G.; Zabala, R. D.; Nassar, N. N.; Franco, C. A.; Alvarado, V.; Cortés, F. B. The effects of SiO2 nanoparticles on the thermal stability and rheological behavior of hydrolyzed polyacrylamide based polymeric solutions. *J. Pet. Sci. Eng.* **2017**, *159*, 841−852.
(17) Rezaei, A.; Abdi-Khangah, M.; Mohebbi, A.; Tatar, A.; Mohammadi, A. H. Using surface modified clay nanoparticles to improve rheological behavior of Hydrolized Polyacrylamid (HPAM) solution for enhanced oil recovery with polymer flooding. *J. Mol. Liq.* **2016**, *222*, 1148−1156.
(18) Zhu, D.; Wei, L.; Wang, B.; Feng, Y. Aqueous hybrids of silica nanoparticles and hydrophobically associating hydrolyzed polyacrylamide used for EOR in high-temperature and high-salinity reservoirs. *Energies* **2014**, *7*, 3858−3871.
(19) Zargartalebi, M.; Kharrat, R.; Barati, N. Enhancement of surfactant flooding performance by the use of silica nanoparticles. *Fuel* **2015**, *143*, 21−27.
(20) Cheraghian, G.; Hendraningrat, L. A review on applications of nanotechnology in the enhanced oil recovery part A: effects of nanoparticles on interfacial tension. *Int. Nano Lett.* **2016**, *6*, 129−138.
(21) Wu, Y.; Chen, W.; Dai, C.; Huang, Y.; Li, H.; Zhao, M.; He, L.; Jiao, B. Reducing surfactant adsorption on rock by silica nanoparticles for enhanced oil recovery. *J. Pet. Sci. Eng.* **2017**, *153*, 283−287.
(22) Farhani, F.; Muhammed, B.; Sabir, A.; Abas, J.; Ali, J. A. Recent advances in application of nanotechnology in chemical enhanced oil recovery: Effects of nanoparticles on wettability alteration, interfacial tension reduction, and flooding. *Egypt. J. Pet.* **2018**, *11*, No. 33.
(23) Rahimi, K.; Adibifard, M.; Hemmati, M.; Shariat Panahi, H.; Gerami, S. Experimentally investigation of the effects of nanoparticles-enriched ASP formulations on the spontaneous imbibition in a fractured sandstone reservoir. *Asia-Pac. J. Chem. Eng.* **2016**, *11*, 98−107.
(24) Xu, D.; Bai, B.; Meng, Z.; Zhou, Q.; Li, Z.; Lu, Y.; Wu, H.; Hou, J.; Kang, W. *A Novel Ultra-Low Interfacial Tension Nanofluid for Enhanced Oil Recovery in Super-Low Permeability Reservoirs*, SPE Asia Pacific Oil and Gas Conference and Exhibition; Society of Petroleum Engineers, 2018.
(25) Suleimanov, B. A.; Ismailov, F.; Veliyev, E. Nanofluid for enhanced oil recovery. *J. Pet. Sci. Eng.* **2011**, *78*, 431−437.
(26) Kamal, M. S.; Adewunmi, A. A.; Sultan, A. S.; Al-Hamad, M. F.; Mehmood, U. Recent advances in nanoparticles enhanced oil recovery: rheology, interfacial tension, oil recovery, and wettability alteration. *J. Nanomater.* **2017**, *2017*, No. 3175.
(27) Betancur, S.; Carrasco-Marín, F.; Franco, C. A.; Cortés, F. B. Development of Composite Materials Based on the Interaction between Nanoparticles and Surfactants for Application in Chemical Enhanced Oil Recovery. *Ind. Eng. Chem. Res.* **2018**, *57*, 12367−12377.
(28) Betancur, S.; Carrasco-Marín, F.; Pérez-Cadenas, A. F.; Franco, C. A.; Jiménez, J.; Manrique, E. J.; Quintero, H.; Cortés, F. B. Effect of Magnetic Iron Core−Carbon Shell Nanoparticles in Chemical Enhanced Oil Recovery for Ultralow Interfacial Tension Region. *Energy Fuels* **2019**, *33*, 4158−4168.
(29) Betancur, S.; Franco, C. A.; Cortés, F. B. Magnetite-silica nanoparticles with a core-shell structure for inhibiting the formation damage caused by the precipitation/deposition of asphaltene. *J. Magnetohydrodyn. Plasma Res.* **2016**, *21*, 289−322.
(30) *Determination of Saturated, Aromatic and Polar Compounds in Petroleum Products by Thin Layer Chromatography and Flame Ionization Detection*; Energy Institute, 2011.
(31) Tuteja, A.; Mackay, M. E.; Narayanan, S.; Asokan, S.; Wong, M. S. Breakdown of the continuum Stokes− Einstein relation for nanoparticle diffusion. *Nano Lett.* **2007**, *7*, 1276−1281.
(32) Kaszuba, M.; McKnight, D.; Connah, M. T.; McNeil-Watson, F. K.; Nobbmann, U. Measuring sub nanometre sizes using dynamic light scattering. *J. Nanopart. Res.* **2008**, *10*, 823−829.
(33) Rouquerol, F.; Sing, K. *Adsorption by Powders and Porous Solids*; Academic San Diego: CA, 2006.
(34) Franco, C. A.; Cortés, F. B.; Nassar, N. N. Adsorptive removal of oil spill from oil-in-fresh water emulsions by hydrophobic alumina nanoparticles functionalized with petroleum vacuum residue. *J. Colloid Interface Sci.* **2014**, *425*, 168−177.
(35) Strother, T.; Lowry, S.; Bravo, B. *Measurement of Dispersed Oil in Water Using an Infrared Analysis Method*; Thermo Fisher Scientific, 2013.
(36) Chun, A. H.; Martin, A. N. Measurement of hydrophile-lipophile balance of surface-active agents. *J. Pharm. Sci.* **1961**, *50*, 732−736.
(37) du Noüy, P. L. An interfacial tensiometer for universal use. *J. Gen. Physiol.* **1925**, *7*, No. 625.
(38) Montoya, T.; Coral, D.; Franco, C. A.; Nassar, N. N.; Cortés, F. B. A novel solid−liquid equilibrium model for describing the adsorption of associating asphaltene molecules onto solid surfaces based on the "Chemical Theory". *Energy Fuels* **2014**, *28*, 4963−4975.
(39) Verdier, C.; Vinagre, H. T.; Piau, M.; Joseph, D. D. High temperature interfacial tension measurements of PA6/PP interfaces compatibilized with copolymers using a spinning drop tensiometer. *Polymer* **2000**, *41*, 6683−6689.
(40) Ko, K. M.; Chon, B. H.; Jang, S. B.; Jang, H. Y. Surfactant flooding characteristics of dodecyl alkyl sulfate for enhanced oil recovery. *J. Ind. Eng. Chem.* **2014**, *20*, 228−233.
(41) Elmendorp, J.; De Vos, G. Measurement of interfacial tensions of molten polymer systems by means of the spinning drop method. *Polym. Eng. Sci.* **1986**, *26*, 415−417.
(42) Betancur, S.; Carmona, J. C.; Nassar, N. N.; Franco, C. A.; Cortés, F. B. Role of particle size and surface acidity of silica gel nanoparticles in inhibition of formation damage by asphaltene in oil reservoirs. *Ind. Eng. Chem. Res.* **2016**, *55*, 6122−6132.
(43) Socrates, G. *Infrared and Raman Characteristic Group Frequencies: Tables and Charts*; John Wiley & Sons, 2004.
(44) Miller, F. A.; Wilkins, C. H. Infrared spectra and characteristic frequencies of inorganic ions. *Anal. Chem.* **1952**, *24*, 1253−1294.
(45) Wahab, R.; Ansari, S.; Dar, M. A.; Kim, Y. S.; Shin, H. S. Synthesis of magnesium oxide nanoparticles by sol-gel process. *Materials Science Forum*; Trans Tech Publications, 2007; pp 983−986.
(46) Farzaneh, F. Synthesis and characterization of Cr2O3 nanoparticles with triethanolamine in water under microwave irradiation. *J. Sci., Islamic Repub. Iran* **2011**, *22*, 329−333.
(47) Álvarez, C. G. P.; Bolaños, P. A. V.; García, C. P. G. Síntesis y caracterización de a-alúmina nanometrica. *Boletín de Ciencias de la Tierra* **2010**, 51−59.
(48) Stuart, B. Infrared Spectroscopy. In *Kirk-Othmer Encyclopedia of Chemical Technology*; Wiley, 2000; pp 1−18.
(49) Bae, H.; Ahmad, T.; Rhee, I.; Chang, Y.; Jin, S.-U.; Hong, S. Carbon-coated iron oxide nanoparticles as contrast agents in magnetic resonance imaging. *Nanoscale Res. Lett.* **2012**, *7*, No. 44.
(50) Carvalho, R. C. Modificación química superficial de carbones mesoporosos activados. In *Aplicaciones en catálisis y adsorción*; DEHESA, 2016.
(51) Nakamoto, K. Infrared and Raman Spectra of Inorganic and Coordination Compounds. In *Handbook of Vibrational Spectroscopy*; Wiley, 2006.
(52) Coates, J. Interpretation of Infrared Spectra, a Practical Approach. In *Encyclopedia of Analytical Chemistry: Applications, Theory and Instrumentation*; Wiley, 2006.
(53) Christ, R. D.; Wernli, R. L., Sr *The ROV manual: a user guide for remotely operated vehicles*; Butterworth-Heinemann, 2013.
(54) De Ferrer, M. P. *Inyección de agua y gas en yacimientos petroliferos*; Ediciones astro data SA: Maracaibo, 2001.
(55) Demissie, H.; Duraisamy, R. Effects of electrolytes on the surface and micellar characteristics of Sodium dodecyl sulphate surfactant solution. *J. Sci. Innov. Res.* **2016**, *5*, 208−214.
(56) Pfeiffer, C.; Rehbock, C.; Hühn, D.; Carrillo-Carrion, C.; de Aberasturi, D. J.; Merk, V.; Barcikowski, S.; Parak, W. J. Interaction of colloidal nanoparticles with their local environment: the (ionic) nanoenvironment around nanoparticles is different from bulk and

DOI: 10.1021/acsomega.9b02372
ACS Omega 2019, 4, 16171−16180

determines the physico-chemical properties of the nanoparticles. *J. R. Soc., Interface* **2014**, *11*, No. 20130931.
(57) Thommes, M.; Kaneko, K.; Neimark, A. V.; Olivier, J. P.; Rodriguez-Reinoso, F.; Rouquerol, J.; Sing, K. S. Physisorption of gases, with special reference to the evaluation of surface area and pore size distribution (IUPAC Technical Report). *Pure Appl. Chem.* **2015**, *87*, 1051−1069.
(58) Griffin, W. C. Classification of surface-active agents by "HLB". *J. Soc. Cosmet. Chem.* **1949**, *1*, 311−326.
(59) Weissmann, M.; Baranton, S.; Clacens, J.-M.; Coutanceau, C. Modification of hydrophobic/hydrophilic properties of Vulcan XC72 carbon powder by grafting of trifluoromethylphenyl and phenylsulfonic acid groups. *Carbon* **2010**, *48*, 2755−2764.
(60) Montoya, T.; Coral, D.; Franco, C. A.; Nassar, N. N.; Cortés, F. B. A novel solid−liquid equilibrium model for describing the adsorption of associating asphaltene molecules onto solid surfaces based on the "chemical theory". *Energy Fuels* **2014**, *28*, 4963−4975.
(61) Aoudia, M.; Al-Shibli, M. N.; Al-Kasimi, L. H.; Al-Maamari, R.; Al-bemani, A. Novel surfactants for ultralow interfacial tension in a wide range of surfactant concentration and temperature. *J. Surfactants Deterg.* **2006**, *9*, 287−293.
(62) Cheraghian, G.; Hendraningrat, L. A review on applications of nanotechnology in the enhanced oil recovery part B: effects of nanoparticles on flooding. *Int. Nano Lett.* **2016**, *6*, 1−10.

DOI: 10.1021/acsomega.9b02372
ACS Omega 2019, 4, 16171−16180